Growth and characterization of InAs epitaxial layer on GaAs(111)*B*

H. Wen,* Zh. M. Wang, J. L. Shultz, B. L. Liang, and G. J. Salamo
Department of Physics, University of Arkansas, Fayetteville, Arkansas 72701, USA
(Received 7 May 2004; revised manuscript received 24 August 2004; published 5 November 2004)

The behavior of InAs deposition on GaAs(111)*B* substrates and the corresponding routes toward strain relaxation have been investigated. InAs growth was for depositions ranging from 2 monolayers to 30 monolayers. Over this deposition range, different routes for strain relaxation caused by the lattice mismatch were observed. The strain relaxed through ragged step edge formation and Ga-In intermixing for low InAs deposition and through the formation of step bunching and dislocations for thicker depositions.

DOI: 10.1103/PhysRevB.70.205307 PACS number(s): 81.15.Hi, 68.35.Bs, 71.55.Eq, 81.16.−c

I. INTRODUCTION

Many investigations have shown that InAs growth on GaAs(100) leads to beautiful three-dimensional (3D) islands under normal growth conditions.[1–3] More recently, similar nanostructures have been observed through InAs deposition on GaAs high-index surfaces.[4–7] In the early 1990s however, it was found that InAs epitaxial growth on GaAs(110) and GaAs(111)*A* could grow as a two-dimensional (2D) surface.[8,9] These results attracted interest in non-(100) surfaces for epitaxial growth. This was especially true for GaAs(111)*A* substrates because of a potentially useful strain-induced piezoelectric field on [111] and an increase in the optical matrix element that arises from a heavier hole mass.[10] Although GaAs(111)*B* has the same piezoelectric properties as GaAs(111)*A*, only a few studies of InAs growth behavior on GaAs(111)*B* have been reported and the results may be viewed as still controversial. For example, both 3D island formation and smooth 2D growth have been reported for InAs deposition on GaAs(111)*B*.[11–13]

In this work, InAs films with different thickness were deposited on GaAs(111)*B* vicinal substrates (cut at 2° towards [2-1-1]) by molecular beam epitaxy (MBE). Reflection high-energy electron diffraction (RHEED) pattern observation, scanning tunneling microscopy (STM) images, and photoluminescence (PL) measurements were used to study the deposition behavior. Different stain relaxation routes and the corresponding surface morphology at different deposition stages were explored.

II. EXPERIMENT

The experiments reported here were performed in a combined MBE-STM ultrahigh vacuum (UHV) system, which is equipped with an optical system that monitors the substrate band edge to give accurate growth temperatures. MBE growth under various growth conditions was monitored *in situ* by RHEED. Growths were carried out on GaAs(111)*B* substrates cut at 2° towards [2-1-1]. Before starting the growth, the native oxide of the GaAs surface was desorbed at 580 °C under 3.7×10^{-6} Torr As_4 flux. This was followed by deposition of a 0.5 μm GaAs buffer layer at a temperature of 600 °C, a growth rate of 0.75 monolayer (ML)/s, and a V/III flux ratio of 7.5. During growth, the RHEED pattern was kept as $(\sqrt{19}\times\sqrt{19})R23.4°$ reconstruction in order to suppress the growth of pyramidlike defects and achieve a smooth GaAs surface.[23] After deposition of the buffer layer, the substrate temperature was cooled to 500 °C for the growth of a InAs epitaxial layer at a growth rate of 0.09 ML/s and a V/III flux ratio of over 40. After InAs being deposited, the temperature was reduced simultaneously under As pressure. The samples were subsequently transferred through an UHV transfer chamber into the STM chamber. Constant current STM images were obtained using a tunneling current of around 0.1 nA and a sample bias of −3.0 V.

III. RESULT AND DISCUSSION

The growth of a smooth buffer layer surface on a conventional GaAs(111)*B* substrate is difficult to obtain due to the formation of defects, such as, pyramid structures and microtwins. It has been reported, however, that nearly atomically flat films can be produced within an extremely narrow window of growth conditions between $(\sqrt{19}\times\sqrt{19})R23°$ reconstruction and high temperature (1×1) reconstruction.[14,15] The restricted growth conditions are in fact the likely reason for the low interest in GaAs(111)*B* as a substrate for epitaxial growth. On the other hand, the use of a GaAs(111)*B* vicinal substrate with a 2° tilt toward [2-1-1] has been demonstrated to be a more favorable choice for smooth homoepitaxial growth over a broad range of growth conditions.[16,17] Figure 1 presents STM images of the GaAs buffer layer surface grown on a vicinal GaAs(111)*B* substrate. The large area STM image shown in Fig. 1(a) indicates that the surface is smooth and without pyramid defects. Most of steps on the surface are monolayer steps and only a few are two or three steps bunched together. The higher resolution STM image shown on Fig. 1(b) indicates the step edges are all straight.

After the buffer layer growth, 2 ML of InAs was deposited. Figure 2 shows the corresponding STM surface images. The large area STM image shown in Fig. 2(a) indicates a perfect two-dimensional mirrorlike surface. The higher resolution image shown in Fig. 2(b) indicates the surface is consistent with monolayer steps toward the [2-1-1] direction. However, the edge of the steps are now all "saw-edge" shaped. The formation of such ragged step edges shown in Fig. 2(b), as opposed to the relatively straight step edge

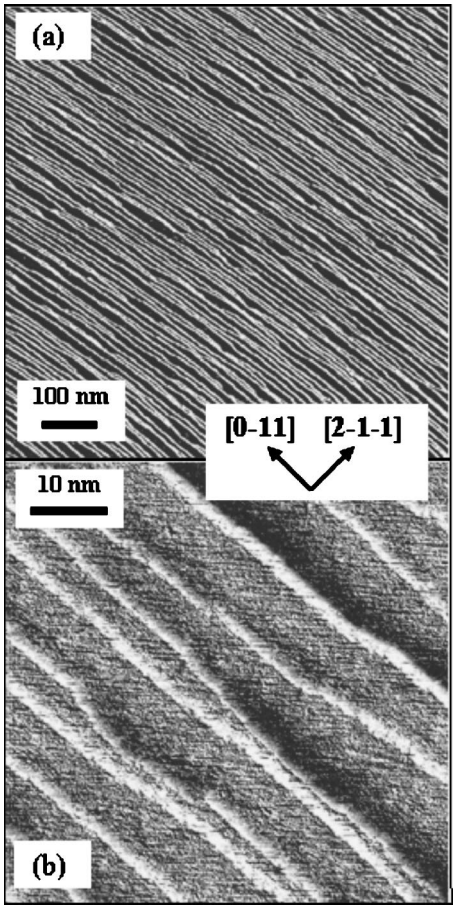

FIG. 1. Buffer layer surface morphology on 2° vicinal GaAs(111)*B* substrate.

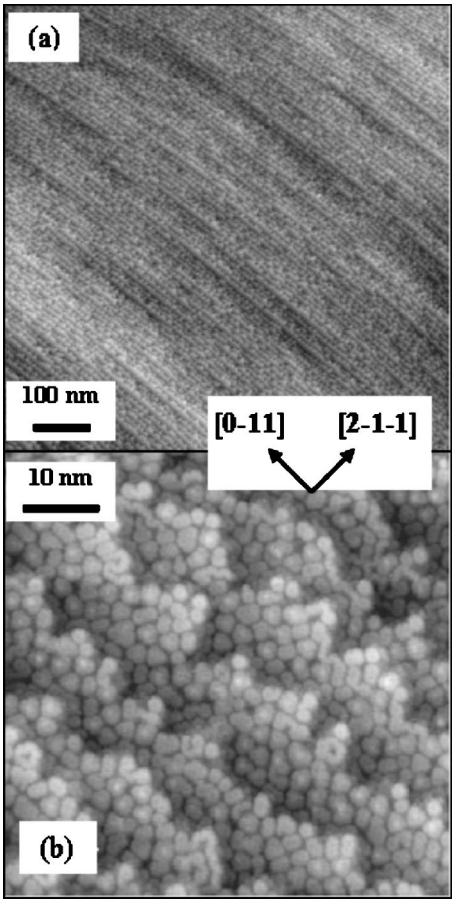

FIG. 2. STM images of InAs 2 ML deposition surface on GaAs(111)*B* substrate.

shown in Fig. 1(b), is due to the fact that the lattice constant of InAs is about 7% larger than that of GaAs. As the step edges changed from straight to ragged, the line length along the step edge is dramatically increased. The longer length offers a way to relieve strain and accommodate a larger lattice constant. Therefore, the ragged step edge is one of the routes for strain relaxation[18] for low deposition of InAs on the GaAs(111)*B* high index surface.

Figure 3 is a high resolution STM image which shows surface reconstruction after the deposition of 2 ML of InAs on a GaAs(111)*B* substrate. The surface is crowded with circular units consisting of 2 to 5 smaller ring elements, which is characteristic of the $(\sqrt{19}\times\sqrt{19})R23.4°$ reconstructure typically found for GaAs homoepitaxial growth on GaAs(111)*B* substrate. The pattern is described as a unit containing six As atoms in the topmost layer corresponding to the six bright lobes in the STM image.[19] Compared to the surface reconstructure of homoepitaxial growth, the $(\sqrt{19}\times\sqrt{19})R23.4°$ reconstructure on the InAs surface is completely disordered, and some of the rings shown in Fig. 3 are open and even become a wormlike structure. This is mainly due to Ga-In intermixing. During InAs deposition on GaAs, some Ga atoms migrate from buffer layer and In atoms from the InAs layer, and intermix. The intermixing leads to alloying of the InAs layer which, in turn, results in disordered reconstruction of the InGaAs surface. Similar observations have been made for the epitaxial growth of InAs on GaAs(100).[20] The surface alloying leads to a reduction in the strain gradient for lattice mismatched systems[21] and provides another route for strain relaxation during InAs deposition on a GaAs(111)*B* substrate. Not only is the disordered reconstruction caused by alloying but also the alloying is partly driven by the reconstruction. The whole process involves

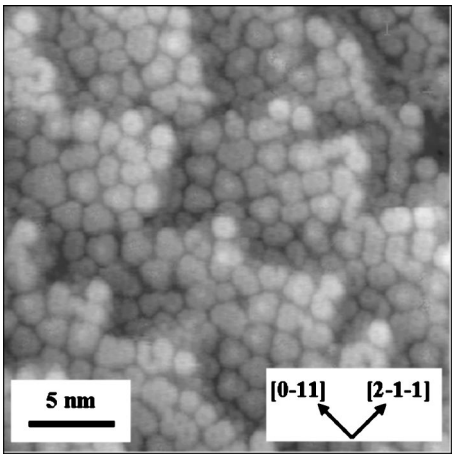

FIG. 3. High resolution STM image for 2 ML InAs deposition surface on GaAs(111)*B*.

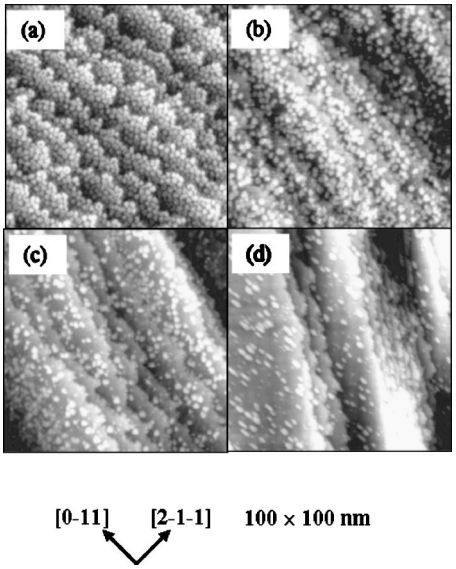

FIG. 4. Surface morphology when InAs deposition on GaAs(111)*B* was (a) 2 ML, (b) 3 ML, (c) 5 ML, (d) 12 ML.

interplay between surface reconstruction, alloying and strain relaxation.[22]

In addition to the investigation of 2 ML InAs deposition, we also deposited 3 ML, 5 ML, and 12 ML of InAs on GaAs(111)*B* under the same growth conditions. Figure 4 shows a comparison of the surface morphologies of the four different InAs depositions. There are three important points that can be drawn from this comparison. First, all four InAs surfaces are two-dimensional with no three dimension structures. In fact, based on RHEED images, even at a thickness of 30 ML, there was no sign of three-dimensional growth. Second, the disorder in the $(\sqrt{19}\times\sqrt{19})R23.4°$ surface reconstructure becomes less as the InAs layer thickness increases, which is consistent with the premise that the disordered $(\sqrt{19}\times\sqrt{19})R23.4°$ surface reconstructure is caused by Ga-In intermixing. Third, step bunching becomes more prominently observed as the InAs layer thickness increases. Studies indicate that when a vicinal surface is under stress, the elastic relaxation around each step causes a logarithmic attraction between steps, leading to step-bunching, regardless of the As flux or step density.[24–26] Therefore, step bunching is another route for stain relaxation for larger InAs deposition on the GaAs(111)*B* surface.

It is well-known that 3D island formation is a dominant strain relaxation mechanism, e.g., InAs growth on GaAs(100). Therefore, the observation of 2D growth up to 30 ML of InAs on vicinal GaAs(111)*B* is surprising. In this case, no InAs islands was observed even on nominal GaAs(111)*B*, except supersize islands due to growth defects. We believe the supersize islands due to growth defects account for the previous claim of 3D InAs growth on GaAs(111)*B*.[13] The observation of 2D InAs growth on GaAs(111)*B* is consistent with the recent idea of the strain-driven facet formation as a mechanism of relaxation.[4,5] According to this strain relaxation mechanism, the occurrence of certain facets bounding InAs islands on GaAs surfaces, indicate that the surface with the same index is stable under

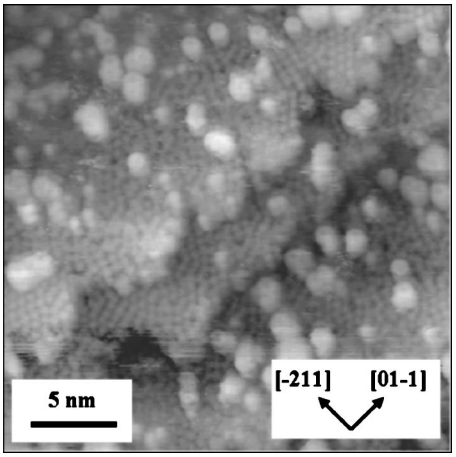

FIG. 5. High resolution STM image for 12 ML InAs deposition surface on GaAs(111)*B*.

strain. InAs growth on GaAs along this direction maintains a 2D mode. Facets with indices of (110) and (111)*A* and (111)*B* have been observed for InAs islands on GaAs surfaces.[4,27] Consistently, the 2D growth mode for InAs growth on GaAs, which has been observed along (110) and (111)*A*,[8,9] should persist along (111)*B*.

Figure 5 shows a high resolution STM image surface after deposition of 12 ML of InAs. Compared to the 2 ML InAs deposition shown in Fig. 3, which is characterized by a disordered $(\sqrt{19}\times\sqrt{19})R23.4°$ reconstructed surface, the surface for 12 ML of InAs deposition is still characterized by a disordered $(\sqrt{19}\times\sqrt{19})R23.4°$ surface reconstruction but cover less of the surface. Instead, most of the surface is now covered by ordered (2×2) reconstruction. This is expected since much less Ga atoms can migrate to the top of a thick surface.

To further investigate the routes for strain relaxation of InAs on GaAs(111)*B*, a GaAs/InAs/GaAs quantum well structure was also fabricated on the GaAs(111)*B* substrate in order to examine PL. The PL measurements were made at a temperature of 12 K using the 532 nm line of Verdi-V10 laser for excitation. In Fig. 6, the PL spectrum shows strong peak values when the InAs thickness was 2 ML and 4 ML.

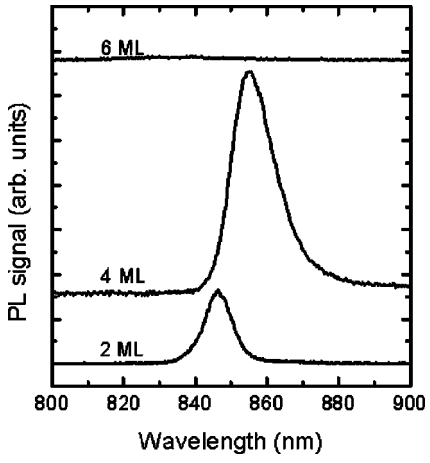

FIG. 6. PL spectra of InAs/GaAs(111)*B* structures with InAs deposition of 2 ML, 4 ML, and 6 ML, respectively.

However, when the InAs thickness was increased to 6 ML, the PL peak disappeared, indicating the density of defects, such as, dislocations became high. The formation of the defects is a result of the release of strain accumulated during deposition. Therefore, dislocation formation is another route for strain relaxation for high InAs deposition on GaAs(111)*B* surface.

IV. CONCLUSION

The behavior of InAs deposition on GaAs(111)*B* substrates and the routes toward strain relaxation during the deposition have been investigated by STM images and PL testing. InAs growth was observed to be two-dimensional without the formation of three-dimensional structures for depositions ranging from 2 ML to 30 ML despite the lattice mismatch. However, over this deposition range, different routes for strain relaxation caused by the lattice mismatch were observed. The strain relaxed through ragged step edge formation and Ga-In intermixing for low InAs deposition and through the formation of step bunching and dislocations for thicker depositions.

ACKNOWLEDGMENTS

The authors acknowledge the funding supports from MRSEC and NSF, especially through Grant No. CA-DMR-0080054-NSF/MRSEC.

*Email address: hwen@uark.edu

[1] Y. Chen, G. H. Li, Z. M. Zhu, H. X. Han, Z. P. Wang, W. Zhou, and Z. G. Wang, Appl. Phys. Lett. **76**, 3188 (2000).
[2] S. Anders, C. S. Kim, B. Klein, M. W. Keller, R. P. Mirin, and A. G. Norman, Phys. Rev. B **66**, 125309 (2002).
[3] Y. I. Mazur, J. W. Tomm, V. Petrov, G. G. Tarasov, H. Kissel, C. Walther, Z. Ya. Zhuchenko, and W. T. Masselink, Appl. Phys. Lett. **78**, 3214 (2001).
[4] Z. M. Wang, H. Wen, V. R. Yazdanpanah, J. L. Shultz, and G. J. Salamo, Appl. Phys. Lett. **82**, 1688 (1997).
[5] H. Wen, Z. M. Wang, and G. J. Salamo, Appl. Phys. Lett. **84**, 1756 (2004).
[6] S. Sanguinetti, M. Guzzi, E. Grilli, G. Panzarini, and M. Henini, Appl. Phys. Lett. **77**, 1982 (2000).
[7] D. I. Lubyshev, P. P. Gonzalez-Borrero, E. Marega, Jr., E. Petitprez, and P. Basmaji, J. Vac. Sci. Technol. B **14**, 2212 (1996).
[8] H. Yamaguchi, M. R. Fahy, and B. A. Joyce, Appl. Phys. Lett. **69**, 776 (1996).
[9] J. G. Belk, J. L. Sudijono, H. Yamaguchi, X. M. Zhang, D. W. Pashley, C. F. McConville, T. S. Jones, and B. A. Joyce, J. Vac. Sci. Technol. A **15**, 915 (1997).
[10] D. L. Smith and C. Mailhiot, J. Appl. Phys. **63**, 2717 (1988).
[11] M. Ilg and K. H. Ploog, Appl. Phys. Lett. **62**, 997 (1993).
[12] S. E. Hooper, D. I. Westwood, D. A. Woolf, S. S. Heghoyan, and R. H. Williams, Semicond. Sci. Technol. **8**, 1069 (1993).
[13] S. B. Schujman, S. R. Soss, K. Stokes, and L. J. Schowalter, Surf. Sci. **385**, L965 (1997).
[14] D. H. Tomich, K. G. Eyink, M. L. Seaford, W. F. Taferner, C. W. Tu, and W. V. Lampert, J. Vac. Sci. Technol. B **16**, 1479 (1998).
[15] D. A. Woolf, D. I. Westwood, and R. H. Wiliams, Appl. Phys. Lett. **62**, 1370 (1993).
[16] X. Marcadet, A. Fily, S. Collin, J. P. Landesman, M. Larive, J. Olivier, and J. Nagle, J. Cryst. Growth **201/202**, 284 (1999).
[17] K. Yang, L. J. Schowalter, B. K. Laurich, J. H. Campell, and D. L. Smth, J. Vac. Sci. Technol. B **11**, 779 (1993).
[18] A. Li, F. Liu, D. Y. Petrovykh, J. L. Lin, J. Viernow, F. J. Himpsel, and M. G. Lagally, Phys. Rev. Lett. **85**, 5380 (2000).
[19] A. R. Avery, E. S. Tok, and T. S. Jones, Surf. Sci. **376**, L397 (1997).
[20] J. G. Belk, C. F. McConville, J. L. Sudijono, T. S. Jones, and B. A. Joyce, Surf. Sci. **387**, 213 (1997).
[21] J. Tersoff, Phys. Rev. Lett. **74**, 434 (1995).
[22] F. Liu and M. G. Lagally, Phys. Rev. Lett. **76**, 3156 (1996).
[23] C. Guerret-Piecourt and C. Fontaine, J. Vac. Sci. Technol. B **16**, 204 (1997).
[24] Y. H. Phang, Z. Zhang, and M. G. Lagally, Phys. Rev. Lett. **75**, 2730 (1995).
[25] F. Liu, J. Tersoff, and M. G. Lagally, Phys. Rev. Lett. **80**, 1268 (1998).
[26] Z. M. Wang, J. L. Shultz, and G. J. Salamo, Appl. Phys. Lett. **83**, 1749 (2003).
[27] T. Suzuki, Y. Temko, and K. Jacobi, Phys. Rev. B **67**, 045315 (2003).